

IDENTIFICATION OF FEM BUCKLING MODES OF THIN-WALLED COLUMNS BY USING CFSM BASE FUNCTIONS

S. ÁDÁNY¹, A.L. JOÓ², B.W. SCHAFER³

¹ *Department of Structural Mechanics, Budapest University of Technology and Economics, Hungary <sadany@epito.bme.hu>*

² *Department of Structural Engineering, Budapest University of Technology and Economics, Hungary <ajoo@vbt.bme.hu>*

³ *Department of Civil Engineering, Johns Hopkins University, Baltimore, MD, USA <schafer@jhu.edu>*

ABSTRACT

The objective of this paper is to demonstrate an approximate method whereby eigen buckling modes from a shell finite element method (FE) analysis of a thin-walled member can be quantified in terms of the fundamental buckling classes, namely, global, distortional, local or other. The buckling classes are defined using the mechanical definitions employed in the constrained Finite Strip Method (cFSM). The cFSM base vectors are used as an approximate basis for the general deformations associated with an arbitrary FE buckling mode. Transformation to the approximate basis introduces error, which is minimized in a vector norm sense. The resulting identification (and its associated error) is sensitive to FE mesh discretization, the selected number of cFSM half-waves considered, and boundary conditions, as shown herein. Overall, the approximate method is shown to provide a potentially powerful means to perform modal identification of arbitrary FE buckling modes.

1. INTRODUCTION

In the behaviour of thin-walled columns buckling has crucial importance. It may take place in various forms, but usually three basic classes of buckling modes are distinguished: global, distortional, and local. Though widely accepted definitions for the classes do not exist, they are usually defined on the basis of in-plane cross-sectional deformations. However, it is not the deformation pattern that makes the distinction important, but rather the post-buckling behaviour. Generally, global buckling has no post-buckling reserve, local buckling potentially has significant post-buckling reserve, and distortional buckling has moderate post-buckling reserve. Existence, or lack thereof, of post-buckling reserve greatly influences the member strength, thus it is important to be able to properly identify an arbitrary buckling mode.

Due to advances in computation, the calculation of buckling modes and critical forces is no longer a challenging task. For thin-walled members, most generally the problem is solved by the finite element method (FEM) using shell elements. However, FEM analysis typically leads to hundreds of buckling modes, most of them apparently interacted from modes of various classes. Given a lack of any quantitative method, the identification is typically done by visual inspection - which as a tiring, but, more importantly, highly subjective process.

A new approach to buckling mode identification is presented in this paper, see also [1]. The method employs a special system of modal base functions that have been recently proposed by the Authors [2-4]. The modal base functions are derived by an appropriate transformation of the base functions of the semi-analytical finite strip method (FSM). The system of transformed base functions are referred to as the cFSM base functions and have the special feature of separating the three (global, distortional and local) mode classes. Thus, if these base functions are used to approximate an arbitrary buckling mode (calculated by any method, e.g., FEM), contribution of the various mode classes can be determined.

2. CFSM BASE FUNCTIONS

Since cFSM is originated from the finite strip method (FSM), its basic feature is that the deformations of the member are expressed via the displacements of the nodes (more exactly: nodal lines), i.e., via the \mathbf{d} displacement vector. Moreover, in accordance with the essence of cFSM, the space of deformation fields determined by the FSM displacement degrees of freedom (DOF) are separated into G, D, L and O sub-spaces corresponding to global, distortional, local and other deformation mode classes, respectively [4]. The separation is based on mechanical criteria, and is realized by defining a constraint matrix, \mathbf{R} , for each deformation mode class. Namely, \mathbf{R}_G , \mathbf{R}_D , \mathbf{R}_L and \mathbf{R}_O represent the transformation from the original FSM nodal system to the modal system of cFSM. Each \mathbf{R} defines a subspace consistent with a given deformation mode class and the columns of \mathbf{R} are the linearly independent base vectors for that sub-space. Since displacement vectors always represent displacement functions, the columns of \mathbf{R} define linearly independent base functions for the sub-space. Since the G, D, L and O subspaces are nearly always multi-dimensional, generally an infinite number of base vectors (functions) is possible to define the subspace. However, if mode contributions are to be calculated, it is strongly advantageous to use orthonormal base vectors (functions). Thus, both orthogonalization and normalization should be performed.

According to cFSM, orthogonalization is completed by solving the constrained eigen-value problem for the member, separately for all four sub-spaces:

$$\mathbf{R}_M^T \mathbf{K}_e \mathbf{R}_M \Phi_M = \Lambda_M \mathbf{R}_M^T \mathbf{K}_g \mathbf{R}_M \text{ or } \mathbf{K}_{eM} \Phi_M = \Lambda_M \mathbf{K}_{gM} \quad (1)$$

where subscript \mathbf{M} may be \mathbf{G} , \mathbf{D} , \mathbf{L} or \mathbf{O} , \mathbf{K}_e and \mathbf{K}_g are the elastic and geometric stiffness matrix for the given member, Φ_M is the matrix of eigen-vectors, Λ_M is the diagonal matrix of the eigen-values, and \mathbf{K}_{eM} and \mathbf{K}_{gM} matrices may be interpreted as the constrained elastic and geometric stiffness matrices, respectively. As a result of Eq. 1, the system of original base vectors, the columns of \mathbf{R}_M , are transformed into a system of orthogonal base vectors, the columns of Φ_M .

Normalization of the orthogonal base systems can be carried out in a variety of ways; here, one of the simplest is selected: vector normalization. Vector normalization yields reasonable results if a regular cross-section discretization is used (other normalizations are briefly discussed for cFSM in [5]). For vector normalization, the $\Phi_{M,i}$ column vectors of the Φ_M matrices are normalized (or in other words: scaled) in a vector sense so that each (orthogonal and normalized) $\varphi_i = \Phi_{M,i} / \|\Phi_{M,i}\|$ vector satisfies that $\varphi_i^T \varphi_i = 1$.

3. APPROXIMATION OF FEM DISPLACEMENTS

Once the φ cFSM base functions are known, it is possible to approximate any δ_{FE} FEM displacement function as a linear combination of the cFSM base functions and c combination factors. The error in this approximation may be expressed as follows:

$$\delta_{err} = \delta_{FE} - \sum c\varphi \quad (2)$$

where $\sum c\varphi$ denotes (symbolically) the linear combination. Following the logic used in normalization of the base functions, the minimization will be completed on the error *vector* (instead of error *function*), by minimizing the vector norm as follows.

$$\min \sqrt{\mathbf{d}_{err}^T \mathbf{d}_{err}} = \sqrt{(\mathbf{d}_{FE} - \Phi \mathbf{c})^T (\mathbf{d}_{FE} - \Phi \mathbf{c})} \quad (3)$$

where Φ is the matrix of orthonormal cFSM base vectors, \mathbf{c} is the vector of unknown combination factors, and \mathbf{d}_{FE} is the displacement vector calculated by FE analysis. Expanding Eq. 3, the function to be minimized may be expressed as:

$$\min f(\mathbf{c}) = \mathbf{d}_{FE}^T \mathbf{d}_{FE} - 2\Phi^T \mathbf{d}_{FE} \mathbf{c} + \mathbf{c}^T \Phi^T \Phi \mathbf{c} \quad (4)$$

which leads to a linear system of equations to be solved for \mathbf{c} :

$$\frac{\partial f(\mathbf{c})}{\partial \mathbf{c}} = 0 \rightarrow \Phi^T \Phi \mathbf{c} = \Phi^T \mathbf{d}_{FE} \quad (5)$$

After calculating the combination factors (elements of \mathbf{c}), p_i participation of an individual buckling mode (or base function) can be calculated. Moreover, taking advantage that within the base functions the various buckling classes (i.e. global, distortional or local) are separated, the p_M participation of a class can be expressed as follows:

$$p_i = |c_i| / \sum_{\text{all}} |c_i| \rightarrow p_M = \sum_M |c_i| / \sum_{\text{all}} |c_i| \quad (6)$$

where c_i is an element of the \mathbf{c} vector, while the M denotes that summation should be performed over all elements of a given mode class. The error of approximation can also be measured, e.g. as the norm of the error vector relative to the norm of the displacement vector (i.e., a “normalized” version of the norm of the error vector)

$$err = \sqrt{\mathbf{d}_{err}^T \mathbf{d}_{err}} / \sqrt{\mathbf{d}_{FE}^T \mathbf{d}_{FE}} \quad (7)$$

4. NUMERICAL RESULTS

To illustrate the application and capabilities of the proposed identification method, a parametric study is completed on a symmetric lipped channel (C-shape) column. The column length is 1200 mm, with a web height of 100 mm, flange width of 60 mm, lip lengths of 10 mm, and thickness of 2 mm. Note, the dimensions are for the mid-line, and sharp corners are employed. Steel material is assumed with a Young's modulus of 210 000 MPa and Poisson's ratio of 0.3. For loading, a uniformly distributed concentric force is applied. Figure 1 illustrates the cFSM base functions by showing the typical in-plane deformed cross-section shapes (i.e., these are the in-plane visualization of the ϕ_i 's).

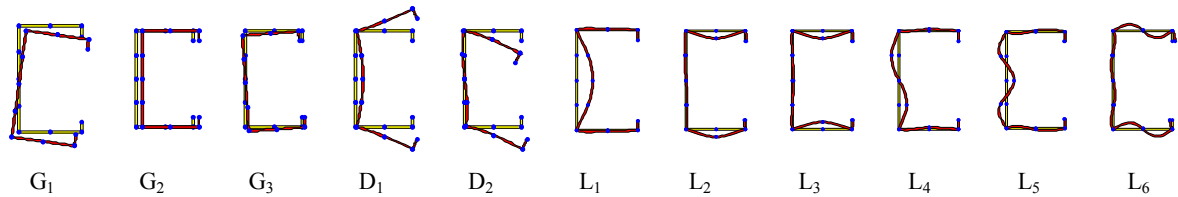


Figure 1: Three global, two distortional and the first six local modes (displaced/deformed cross-sections)

The FE calculations are conducted in ANSYS [6], using 4-node, 24-DOF shell elements in a highly regular (rectangular) mesh. The longitudinal dimension of the finite elements is constant along the member length, and is defined so that the aspect ratio of all the shell elements is close to 1. In the numerical studies presented herein the following parameters were considered: (i) cross-section discretization, (ii) minimum wave-length of the base functions, and (iii) different boundary conditions.

Four different cross-section discretizations are used, denoted by the numbers of sub-nodes within the flanges, web and lips, respectively, e.g., 2-4-1 implies 2 sub-nodes in each of the flanges, 4 in the web, and 1 in each of the lips, which totals to 16 nodes or 15 elements in the cross-section. The considered cases are: 1-3-0, 2-4-1, 3-5-1, and 4-6-2, which lead to the following numbers of displacement degrees of freedom (DOF): 2442, 5088, 7410 and 11376.

Theoretically, the longitudinal distribution of the cFSM base functions can be an arbitrary number of sine half-waves. Practically, the maximum half-wavelength to be considered is equal to the member length. The minimum half-wavelength is considered as a parameter, expressed as the ratio of the minimum half-wavelength considered to the length of a finite element. In the presented study $1\times$, $2\times$, ... $6\times$ are employed, where $q\times$ implies a minimum cFSM half wave-length equal to $q\times$ the finite element length, and smaller q implies a larger number of cFSM base functions. Thus, the number of applied base functions significantly varied in the presented studies, ranging from 264 ($1-3-0$, $6\times$) to 7488 ($4-6-2$, $1\times$).

Finally, five boundary conditions (BC) are investigated. In the case of 'FSM' boundary conditions, the nodes at the supports are restricted from translation, but rotation and longitudinal warping is left free. (Note, this BC exactly corresponds to FSM with a single half-wave along the length; for multiple half-waves FSM-like BC would be different.) The other boundary conditions include 'GF-LP' which represents globally fixed, locally pinned end restraints, 'GF-LF' which corresponds to both globally and locally fixed condition, while in the case of 'LW' and 'LF' options only either the web or the flanges are globally fixed and locally pinned (i.e., restrained against translations but free to rotate). It is worth noting that the applied cFSM base functions are all sine functions in the longitudinal direction, thus they

violate many of the considered boundary conditions. However, as shown here, these same cFSM base functions are able to reasonably approximate the FE displacements in the mid length of the columns for many buckling modes and thus still provide useful identification.

For all of the analyzed cases the first 50 FEM buckling modes were calculated. This covers those modes where the buckling load is smaller than (approximately) 3 times the minimum (first) buckling load. For each buckling mode the cFSM modal identification approximation as described herein is performed. The accuracy of the cFSM approximation is measured by (i) error, as defined in Eq. (7), (ii) the average error of the first n cases (e.g., where $n = 1..50$), and (iii) the number of observations (among the first 50 modes) with an error $>5\%$.

Results for selected modes are presented in Table 1 where the G, D, L and O participations, as well as the calculated error, are given for 8 FE buckling modes. Table 1 results are calculated considering FSM-like end restraints, 3-5-1 cross-section discretization, and $3\times$ for the cFSM minimum wave-length. In this case, $3\times$ implies a maximum of 21 half-waves along the member length. The corresponding deformed shapes are presented in Figure 2: both FEM solutions (\mathbf{d}_{FE}) and their cFSM approximations ($\Phi\mathbf{c}$) are shown.

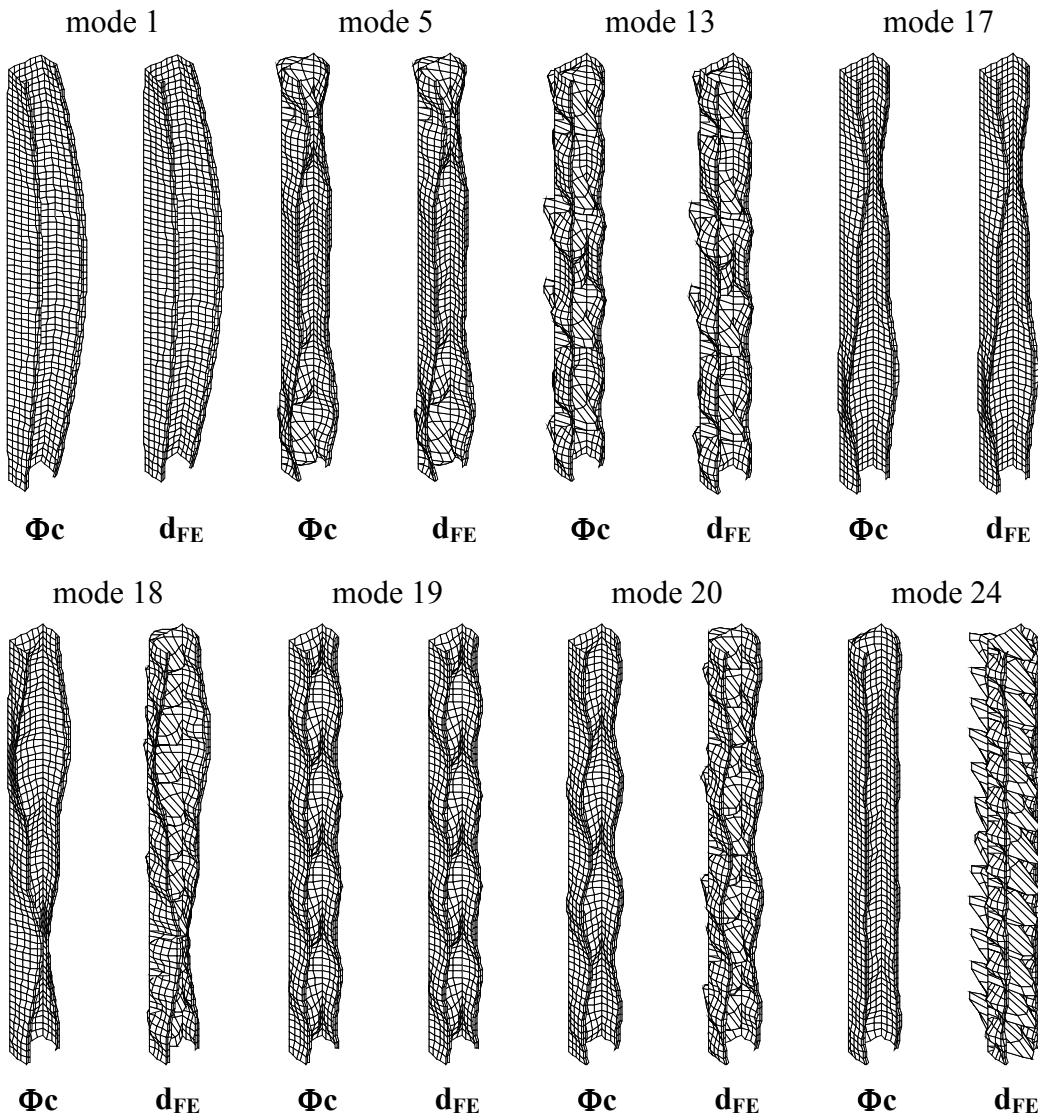


Figure 2: cFSM approximation ($\Phi\mathbf{c}$) of FE eigenmodes (\mathbf{d}_{FE}) for FE with FSM-like end restraints

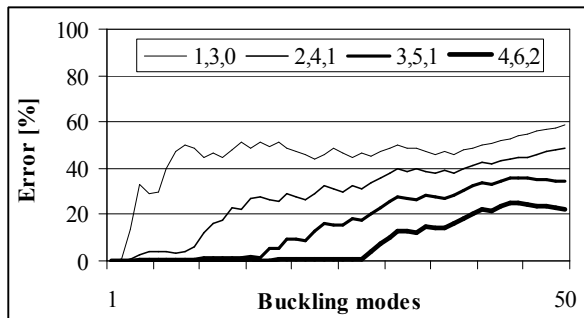
FE mode nr	1	5	13	17	18	19	20	24
G	85.9 %	0.5 %	0.2 %	1.3 %	1.1 %	0.6 %	1.1 %	3.3 %
D	5.5 %	38.4 %	8.6 %	82.5 %	64.1 %	26.7 %	36.8 %	28.8 %
L	0.2 %	58.2 %	88.7 %	12.7%	31.4 %	68.1 %	56.8 %	62.3 %
O	8.4 %	2.9 %	2.5 %	3.5 %	3.4 %	4.6 %	5.4 %	5.5 %
error	0.0 %	2.7 %	1.0 %	0.7 %	74.9 %	1.8 %	89.0 %	99.5 %

Table 1: GDLO participations for the selected modes

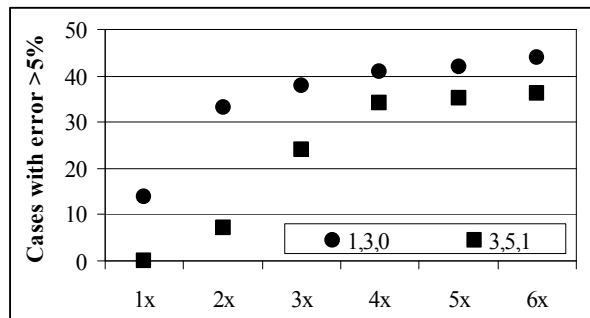
For many of the modes the cFSM approximation is excellent, as both the deformed shapes of Figure 2 and small error in Table 1 indicates (see, e.g., modes #1, #5, #13, #17 and #20). Further, the GDLO participations are in accordance with the engineering expectations: mode #1 is clearly global (flexural-torsional), #17 is dominantly distortional, #13 is local, and #5 and #19 are mixed local-distortional modes. However, cases also exist with significant errors, as can be seen in both the deformed shapes of Figure 2 and error values of Table 1. From Figure 2 it is clear that both #18 and #20 are mixed local and distortional modes, but in neither case is the cFSM approximation able to reproduce the small local waves. This is even more evident in mode #24, which is clearly a local buckling mode with 24 longitudinal half-waves, therefore the applied maximum 21 longitudinal waves in the cFSM base functions are simply not enough to properly handle this buckling mode.

For FSM-like end restraints sensitivity of the cFSM modal identification to mesh discretization and minimum cFSM half-wavelength is summarized in Figure 3a and b, respectively. Figure 3a shows that finer cross-section discretization significantly enhances the accuracy of the approximations, but higher modes tend to have larger error regardless. Considering that higher modes typically include buckling modes with smaller wave-lengths, it is hypothesized that in some cases the source of the error is the limited accuracy of the FEM displacements due to the selected mesh density. Of course, the selected mesh density highly depends on how many and what type of buckling modes are to be identified.

Figure 3b highlights the importance of the number of cFSM base functions considered. As smaller wave-length base functions are added, the number of erroneous cases decreases, especially in the higher buckling modes where small wave-length modes are more likely to occur. The results suggests that if the cFSM base functions are to provide a reasonable approximation of higher FE modes the minimum half-wavelength of the cFSM base functions should not be greater than $2\times$ to $3\times$ of the finite element longitudinal length, and certainly no longer than that of the buckling half-wavelength of the modes that are desired to be identified.



(a) mesh discretization



(b) minimum half-wavelength

Figure 3: Sensitivity of cFSM approximation for FSM-like end restraints

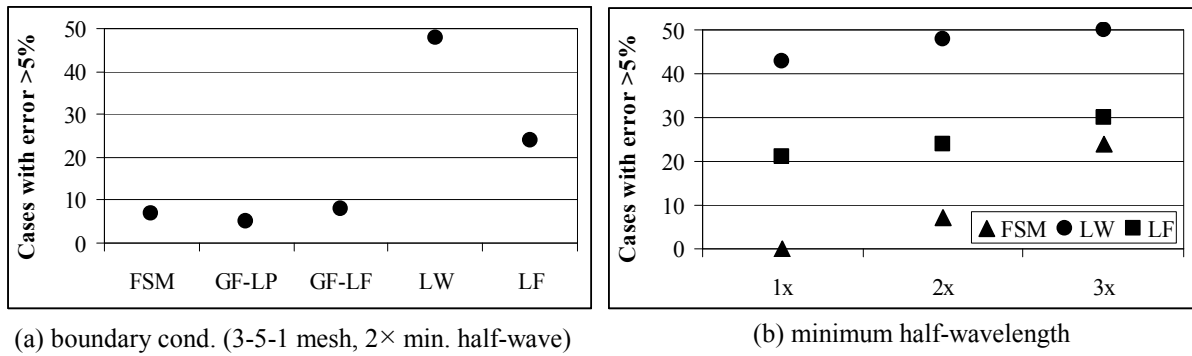


Figure 4: Sensitivity of cFSM approximation for other end restraints

The sensitivity of the cFSM modal identification approximation to boundary conditions (end restraints) and the minimum half-wavelength of the cFSM base vectors is shown in Figure 4. Figure 4a shows that mode identification works for various BC-s, with the definite exception of LW option where only the web is supported, and Figure 4b shows that the selected minimum half-wavelength for the cFSM base functions has significant effect on the accuracy. It must be mentioned, however, that increasing the number of cFSM functions (by decreasing the minimal wave-length) may lead to “parasite” solutions: a relatively small error may be achieved while the identification is clearly unrealistic. This phenomenon occurs frequently in the combination of options LW and 1x.

Finally, in Figure 5 the proposed approximate identification of the FE solution is compared with the cFSM solution itself (as implemented in CUFSM [7,8]). Here the model with FSM-like boundary conditions, 3-5-1 discretization, and 3x minimum half-wavelength is employed. A buckling half-wavelength is manually assigned to each of the 50 modes: for some modes e.g., #1, #19 this is readily apparent, for other modes, e.g., #5, more judgment is required and in some cases no single half-wavelength can be assigned. Buckling stresses and dominant half-wavelengths predicted by the FE and the FSM models are nearly identical, see Figure 5a. Modal participation plot (Figure 5b) highlights some of the additional information contained in the FE models. In the FSM model only one buckling mode can exist at a given half-wavelength, but FE models may have different half-wavelengths superposed (e.g., mode #18), thus the modal participation shows some scatter about the traditional cFSM predictions.

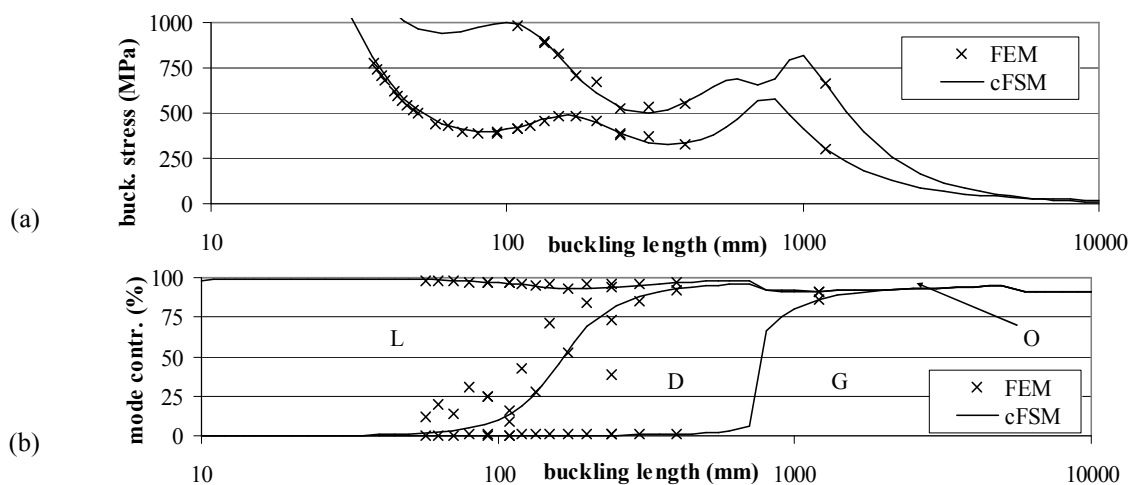


Figure 5: Comparison of (a) buckling stress and (b) mode participation as a function of half-wavelength

5. CONCLUSIONS

An arbitrary buckling mode of a thin-walled member predicted using a shell finite element model may be quantitatively identified in terms of global, distortional, local, or other deformations (mode classes) through the use of the approximate base vectors defined by the constrained Finite Strip Method (cFSM). Through a parametric study of a cold-formed steel lipped channel column the resulting modal identification is shown to be excellent, even for modes with different wavelengths and cross-section deformations (e.g., local and distortional) superposed. Sensitivity to end restraints, finite element (FE) mesh discretization, and the minimum half-wavelength employed for the cFSM base vectors is explored. FE Mesh discretization must be fine enough, and the cFSM base vectors must employ a small enough half-wavelength, to adequately resolve the buckling deformations. The identification works with the least error for FSM-like (locally simply supported) boundary conditions, but can be applied to different end restraints, too. Research work is underway to explore the accuracy of the approximate identification methods to thin-walled members with holes.

ACKNOWLEDGEMENTS

The work has been conducted under the partial support of the OTKA K62970 and T049305 projects of the Hungarian Scientific Research Fund, and the János Bolyai Research Scholarship of the Hungarian Academy of Sciences. This material is based in part upon work supported by the U.S. National Science Foundation under Grant No. 0448707. Any opinions, findings, and conclusions or recommendations expressed in this material are those of the authors and do not necessarily reflect the views of the U.S. National Science Foundation.

REFERENCES

- [1] Ádány, S, Joó, A.L., Schafer, B.W.: Approximate identification of the buckling modes of thin-walled columns by using the cFSM modal base functions; Proceedings of Int. Colloquium on Stability and Ductility of Steel Structures (SDSS), Lisbon, Portugal, Sept 6-8, 2006), IST Press, 197-204.
- [2] Ádány S., Schafer B.W.: Buckling mode decomposition of single-branched open cross-section members via finite strip method: derivation; Thin-Walled Structures, 44(5), 563-584, 2006.
- [3] Ádány S., Schafer B.W.: Buckling mode decomposition of single-branched open cross-section members via finite strip method: application and examples; Thin-Walled Structures, 44(5), 585-600, 2006.
- [4] Ádány S., Schafer B.W.: A full modal decomposition of thin-walled, single-branched open cross-section members via the constrained finite strip method; J of Constructional Steel Research, 64/1, 2008, pp 12-29.
- [5] Ádány, S., Silvestre, N., Schafer, B.W., Camotim, D.: "Buckling mode identification of thin-walled members: a comparison between cFSM and GBT approaches", *Proceedings of the Fifth Int. Conference on Coupled Instabilities in Metal Structures (CIMS 2008)*, June 23-25, 2008, Sydney, Australia. (submitted)
- [6] ANSYS Release 9.0 Documentation, Ansys Inc., 2004.
- [7] Schafer B.W., Ádány S.: Buckling analysis of cold-formed steel members using CUFSM: conventional and constrained finite strip methods; Proceedings of the 18th International Specialty Conference on Cold-Formed Steel Structures, Orlando, USA, October 26-28, 39-54, 2006.
- [8] CUFSM: Elastic Buckling Analysis of Thin-Walled Members by Finite Strip Analysis; CUFSM v3.12, 2006. <http://www.ce.jhu.edu/bschafer/cufsm>